BEARING-PAD/PRESSURE-TUBE RUPTURE EXPERIMENTS

R.G. Moyer, D.B. Sanderson, R.W. Tiede and H.E. Rosinger
AECL Research-Whiteshell Laboratories
Pinawa, Manitoba, Canada R0E 1L0
(204) 753-2311

ABSTRACT

The behaviour of a CANDU[1] pressurized heavy water reactor fuel channel during a postulated loss-of-coolant accident with coincident loss-of-emergency-core cooling is being studied at AECL-Whiteshell Laboratories. In some of these postulated accidents, the pressure tube is predicted to become completely dry in a matter of seconds after flow stagnation occurs. As the pressure-tube depressurizes, the fuel cladding temperatures in the bundle can easily exceed 1000°C. Most of the pressure-tube circumference will be heated by thermal radiation, except at spots where the bearing pads are in contact with the pressure tube. Here, conduction and thermal radiation are the dominant modes of heat transfer. Therefore, local hot spots can develop on the pressure tube under the bearing pads. Whether the pressure tube would fail at these hot spots depends on the localized temperature and pressure transients it experiences.

Experimental results to date, using electrically heated fuel element simulator bundles, have shown that localized hot spots created by bearing-pad contact do not result in significant local strain on the pressure tube during ballooning. Tests were done in steam and simulated steam atmospheres using "as-received," "worn" and the modified "T-pad" bearing pads with similar results. Hence, the probability of pressure-tube failure during ballooning does not appear to be influenced by localized hot spots caused by bearing pads of overheated bundles for the range of experimental conditions studied.

This experimental program was funded by the CANDU Owners Group (COG).

1. INTRODUCTION

In the analysis of postulated Loss-of-Coolant Accidents (LOCA) with coincident Loss-of-Emergency-Core Cooling (LOECC), the thermal-mechanical behaviour of the fuel channel must be understood. Fuel bundles in a CANDU pressurized heavy-water reactor rest on the inside surface of the horizontal pressure tube in the fuel channel. The 0.5-m-long bundles have spacer pads between the individual fuel elements and bearing pads on the outermost ring of elements supporting the weight of the bundle in the pressure tube. We need to determine if pressure-tube failure could result when a local "hot spot" develops at the bearing-pad/pressure-tube contact surface.

The objective of this experimental program is to study the influence of hot bearing pads on the thermal-mechanical behaviour of a ballooning pressure tube. The data from the experiments will support the validation of computer codes used to analyze reactor safety.

---

[1] CANadian Deuterium Uranium, registered trademark at AECL.

The experimental program was divided into three series:

1. Series 1 consisted of four experiments in a steam environment. They examined the influence of power and pressure on the hot spots developed under the bottom bearing pads during pressure tube heat-up and ballooning.

2. Series 2 consisted of two experiments in a simulated steam environment (25% O_2 and 75% Ar) designed to eliminate the problem of steam condensate influencing the temperature gradients in the test section.

3. Series 3 consisted of three experiments performed with three distinctly different bearing pads to determine the influence of bearing-pad types on the thermal-mechanical behaviour of the pressure tube.

This paper describes the results from these experiments.

2. MATERIALS AND METHODS

2.1 Experimental Apparatus

The apparatus consisted of a 1.2-m-long section of autoclaved Zr-2.5 Nb pressure tube positioned concentrically inside a 1.1-m-long Zr-2 calandria tube (Figure 1). The annulus between the pressure and calandria tubes was filled with CO_2 and the calandria tube was surrounded by heated water in an open tank. The pressure tube was connected to a blowdown tank through a line containing a fast-acting hydraulic valve. The blowdown tank was heated to the saturation temperature (for the Series 1 experiments) to maintain pressure after blowdown. For Series 2 and 3 experiments, the hydraulic valve was opened and the blowdown tank helped maintain test-section pressure during the ballooning phase of the experiment.

A cross section of the test section is shown in Figure 2. The fuel element simulators (FESs) were arranged to represent the outer ring of 16 fuel elements in a typical 28-element CANDU fuel bundle. The heater filaments for the fuel element simulators were 6-mm-diameter tungsten-carbide-coated graphite rods, 1100 mm in length. High-purity alumina (Al_2O_3) insulators separated these filaments from the 15.2-mm outer diameter Zr-4 cladding. The cladding had a ring of bearing and spacer pads in five axial locations: at the axial centre of the heater bundle, as well as, 197 and 304 mm on either side of centre. The bearing pads at the central ring were brazed to the cladding so the heat transfer coupling was typical of CANDU fuel. Tungsten weight cans within the bundle provided representative mass per unit length of CANDU fuel bundles (49.4 g/mm).

Experiments 1 to 7 inclusive had "as received" bearing pads at the central bearing-pad ring. These bearing pads were slightly concave in the axial direction and contact with the pressure tube was mainly at the ends (Figure 3a). Experiment 8 had a simulated "worn" bearing pad at the central bottom location (Figure 3b). This simulated the expected wear of bearing pads after extended reactor operation. The "worn" bearing pad had a slightly convex axial profile, and contact with the pressure tube was greatest at the centre. Experiment 9 used the modified "T-Pad" design at the central bottom bearing-pad location (Figure 3c). These bearing pads had a reduced cross section from the cladding to the pressure-tube surface.

2.2 Instrumentation

All 16 fuel element simulators were connected in parallel to a DC power supply. Thermocouples, used to monitor test section temperatures, were typically configured as: three inside the bottom fuel element simulator, 12 on the fuel element simulator cladding, 30 on the outside surface of the pressure tube, and six on the outside surface of the calandria tube.

The three thermocouples located inside the bottom fuel element simulator had 0.25-mm-diameter C-type (tungsten-rhenium) sensing elements threaded through double bore alumina (Al_2O_3) insulators inside a 1.5-mm-diameter tantalum sheath. The wires of these thermocouples were twisted together and fused at one end to form a thermocouple junction. The tantalum sheaths (with thermocouple inside) were threaded through holes in the Al_2O_3 pellets in the bottom fuel element simulator.

Cladding thermocouples were magnesium oxide (MgO) insulated R-type (platinum-rhodium) thermoelements inside 1.0-mm outer diameter Inconel sheaths. The individual wires were slightly separated and spot welded directly onto the surface of the fuel element simulator cladding or bearing pad.

The thermocouples on the pressure tube were 0.5-mm outer diameter Inconel-clad, K-type (chromel-alumel) with magnesium oxide insulation. The thermocouples on the calandria-tube surface were fiberglass insulated K-type with wire diameters of 0.13 mm. In both cases the separated sensing wires were spot-welded directly onto the calandria or pressure-tube surfaces. A typical arrangement of thermocouples attached to the outside surface of the pressure tube (under the central bearing pad) is shown in Figure 4. This thermocouple grid was used to measure the hot spots in the vicinity of the bottom bearing pads.

Relative displacement of the pressure tube with respect to the calandria tube was monitored by top and bottom Linear Variable Differential Transformers (LVDTs) (Figure 4). A third LVDT was added on the bottom (Tests 8 and 9) to measure the ballooning between bearing-pad rings. In these two tests, ballooning and contact times on the bottom of the pressure tube could be compared at the central bearing-pad ring and between the bearing-pad ring located 197 mm from the centre.

2.3 Experimental Procedure

Table 1 lists the test parameters for the three test series.

Table 1

Summary of Experimental Conditions

Test Number	Pressure-Tube Pressure (MPa gauge)	Pressurizing Medium	Test Section Power Per Element (kW/m)	Test Section Power Total (kW)
Series 1 Experiments				
1	2-3	Steam	4.1	72
2	3-3.5	Steam	8.3	146
3	6	Steam	5.0	88
4	6	Steam	8.4	148
Series 2 Experiments				
5	3	Ar-25% O_2	8.1	142
6	6	Ar-25% O_2	7.7	135
Series 3 Experiments				
7	3	Ar-25% O_2	8.1	140
8	3	Ar-25% O_2	8.5	140
9	3	Ar-25% O_2	8.0	140

The experimental procedure for the three series of experiments was as follows:

1) The fuel element simulators were pressurized on the inside with helium. The helium pressure was maintained roughly 1 MPa lower than the pressure-tube pressure to provide a constant differential pressure across the cladding throughout the test.

2. The water surrounding the calandria tube was heated to the required temperature and stirrers turned on to circulate the water.

3. The annulus between the pressure and calandria tubes was purged with CO_2 and maintained slightly above atmospheric pressure throughout the test.

4. The experiments in Series 1 and the first experiment of Series 2 started the high power heat-up stage from an initial pressure-tube temperature of approximately 300°C. During the preheating to 300°C, only selected fuel element simulators near the bottom of the pressure

tube were powered. This procedure minimized the circumferential temperature gradient on the pressure tube and helped reduce condensation on the bottom of the pressure tube in the Series 1 experiments.

Experiments 6 through 9 did not have an initial preheat-up stage. High power heat-up began directly from a pressure-tube temperature that matched the temperature of the water surrounding the calandria tube.

5. Pressure-tube pressure was increased to the desired pressure and held constant throughout the experiment.

6. Test section power was ramped from 0 to full power over 50 to 90 s and then remained constant throughout the test.

7. Power was decreased and the test terminated when the pressure tube had fully contacted the calandria tube and stable nucleate boiling was observed on the calandria tube.

3. RESULTS

3.1 Summary of Results

The results from experiments 1 to 9 will be summarized, followed by summaries of each of the three test series. For each test, the test section was pressured and the power ramped from 0 to the desired power (Table 1). This power caused the fuel element simulator temperatures to increase and to radiate energy to the surrounding pressure tube. The resultant pressure-tube heat-up rates for the various experiments are presented in Table 2. These rates were calculated prior to ballooning as heat-up rates decreased slightly during the ballooning phase of the experiment.

When the pressure-tube temperatures increased above approximately 600°C, the pressure tube started to balloon. This deformation continued until the pressure tube ballooned into contact with its surrounding water-cooled calandria tube and subsequently cooled.

Table 2

Summary of Major Experimental Results

Test	Pressure-Tube Heating Rate (^{0}C/s)	Pressure-Tube/Calandria-Tube First Contact		Pressure-Tube Strain*	
		Temperature (°C)	Location	Under Bottom Bearing Pad (local)** (%)	Between Bearing Pads (global)*** (%)
SERIES 1 EXPERIMENTS					
1	3.4	765	Top	<1	<1
2	7.6	785	Top	<1	<1
3	3.8	670	Bottom	12	12
4	7.4	740	Top	9	8
SERIES 2 EXPERIMENTS					
5	7.7	755	Bottom	115	22
6	7.4	-	-	7	5
SERIES 3 EXPERIMENTS					
7	8.6	770	Top	4	7
8	8.2	755	Bottom	8	9
9	8.9	770	Top	12	12

* Strain = ln [original wall thickness/final wall thickness]
** Local = directly under the bearing pad
*** Global = in the vicinity of the bottom bearing pads

In most of the experiments, free convection caused significant temperature gradients to develop on the pressure-tube circumference during heating. The top of the pressure tube was typically 40 to 85°C hotter than the bottom (Table 3) at the central bearing-pad ring. Temperature gradients caused by free convection were generally higher between the bearing-pad rings than at the bearing-pad rings. A typical temperature history between bearing-pad rings (Test 7 shown) is given in Figure 5a. This top-to-bottom circumferential temperature gradient caused most of the strain to occur in the upper half of the pressure tube (Figure 5b).

Table 3

Summary of Pressure-Tube and Bearing-Pad Induced Temperature

Test	Pressure-Tube Temperature Gradients				Localized Hot Spot Under Bearing Pad (°C)
	Circumferential		Axial		
	Maximum (°C)	At PT/CT* Contact (°C)	Maximum (°C)	At PT/CT Contact (°C)	
SERIES 1 EXPERIMENTS					
1	260	230	-	-	15
2	115	115	60	40	15
3	40	35	90	15	10
4	60	40	40	25	10
SERIES 2 EXPERIMENTS					
5	125	85	100	6	20
6	80	65	125	80	10
SERIES 3 EXPERIMENTS					
7	40	20	95	15	10
8	90	50	170	15	35
9	75	70	100	55	15

* PT/CT = Pressure Tube/Calandria Tube

The large top-to-bottom gradients of the pressure tube in Tests 1 and 2 were caused by steam condensate along the bottom of the pressure tube during a large portion of the heat-up phase. The top-to-bottom circumferential gradients caused most of the pressure-tube strain to occur in the upper half of the tube. The bottom of the pressure tube, moved into calandria-tube contact with negligible strain.

Small localized hot spots developed on the pressure tube, directly below the bottom bearing pads in each experiment. These hot spots were caused by the extra heat transferred from the fuel element simulators to the pressure tube via conduction through the bearing pads. Adjacent bearing pads at similar axial locations smoothed out the circumferential temperature gradients, resulting in a band of high temperatures at each bearing-pad ring location. As a result, axial temperature gradients away from the bearing-pad ring were significantly larger than circumferential gradients at the bearing-pad ring (Figure 6). Maximum recorded axial- and circumferential-temperature gradients on the outside surface of the pressure tube in the vicinity of the bottom bearing pads are given in Table 3. The shapes of these gradients are similar to that shown for Test 7 in Figure 6.

3.2 Series 1 - Tests Performed in Steam

The four experiments in Series 1 included two low-pressure tests and two high-pressure tests with low and high bundle power levels. The bearing-pad induced hot spots in these tests were approximately 10 to 15°C above the temperature of the pressure tube between pads. This increased temperature did not cause significantly increased local strain under the bottom bearing pads during ballooning. The high-power tests had higher heat-up rates and the temperature difference between the bottom bearing pad and the pressure tube was higher than the low-power experiments. Changes in test pressure did not appear to have a strong influence on bearing-pad hot spots.

The heat-up rates of the bottom bearing pad and the pressure tube changed during the ballooning phase of the experiments. The thermal gradient from the bottom fuel element simulator to the pressure tube throughout the heat-up and ballooning phases (Test 4) is shown in Figure 7. The differential temperature between the bearing pad and the pressure tube increased during early heat-up, then remained relatively constant until the pressure tube started to balloon (time = 105 s). As ballooning progressed, the heat-up rate of the bearing pad increased and the heat-up rate of the pressure tube decreased. These heating rate changes suggested the contact conductance between the bearing pad and the pressure tube decreased during the ballooning phase.

One of the problems with steam pressurization (Series 1 tests) was the presence of steam condensate on the inside bottom of the pressure tube. Steam condensed on the water-cooled end seals, collected on the bottom and entered the heated test section area from each end. Power was applied to the bottom fuel element simulators to prevent condensation but this procedure caused axial and circumferential gradients within the heater bundle that may have affected gradients on the pressure tube. For this reason, the Series 2 and 3 experiments were pressurized with simulated steam (gas mixture of 75% Ar and 25% O_2).

3.3 Series 2 - Tests Performed in Simulated Steam

The two experiments in Series 2 used high bundle power with 3 and 6 MPa pressure-tube pressure.

One of the objectives of Test 5 was to access the effect of bearing-pad hot spots when the bottom portion of the pressure tube had the highest strain during the ballooning phase. For this reason, the bottom of the pressure tube in experiment 5 was preferentially heated before high power heat-up. This imposed gradient resulted in a bottom pressure-tube temperature approximately 125°C hotter than the top at the start of the ballooning phase. This caused greater wall reduction on the bottom of the pressure tube during the ballooning phase of the experiment (Figure 8). The large global pressure-tube strain (~22%) in the vicinity of the bottom bearing pads, combined with the local bearing-pad hot-spot (~20°C) on the bottom, caused 115% localized strain directly under the central bottom bearing pad. Thus, a relatively modest hot spot is sufficient to cause considerable localized strain during ballooning when the global strain in this location exceeds approximately 20%.

3.4 Series 3 - Effect of Bearing-Pad Design and Wear

Three experiments were performed with similar experimental conditions but with different bearing pads at the central bearing-pad ring. Tests 7, 8 and 9 had "as-received", "worn" and "T-Pad" bearing pads, respectively, at the central bottom bearing-pad locations. These tests were designed to show the effect bearing-pad wear and design changes have on the thermal interaction with the pressure tube under similar test conditions.

Two-dimensional and three-dimensional temperature profiles during Test 7 are shown in Figures 6(a) and (b). These profiles are compared with the profiles of Test 8 shown in Figures 9(a) and (b). The profiles were obtained from the grid of thermocouples on the pressure tube in the vicinity of the central bottom bearing pad.

The contours of Test 7 ("as-received" bearing pads) show a band of high pressure-tube temperatures opposite the ring of bearing pads. This band had slight hot spots directly under the bearing pads of less than 10°C. This result was similar to the temperature profiles obtained in Test 9 using the new "T-Pad" bearing pads. One of the reasons for the minimal bearing-pad induced hot spot is related to its contacting surface. The "as-received" bearing pad has a smaller radius than the inside surface of the pressure tube in the circumferential direction. Also, the bearing-pad surface facing the pressure tube is slightly concave in the axial direction (Figure 3). Thus, most of the metal-to-metal contact with the pressure tube occurred near the ends of the bearing pad.

The abrasion process used to produce a simulated "worn" bearing pad resulted in a slightly convex profile in the axial direction. This produced better mechanical contact and thus a significantly hotter hot spot directly under the bearing pad (Figure 9). The axial temperature gradient away from the bearing-pad ring was also greater than for an "as-received" bearing pad. Both the bearing-pad hot spots and the axial temperature gradient decreased substantially during the ballooning phase. There was no significant local pressure-tube wall thinning under the bottom bearing pads following ballooning contact.

4. DISCUSSION

4.1 General Overview

In general, the axial and circumferential temperature gradients in these experiments developed early in the heat-up phase. These included gradients in the fuel element simulator bundle, gradients on the pressure tube and local gradients in the vicinity of the bottom bearing pads. The temperature gradients did not change substantially during mid-to-late heat-up. The pressure-tube temperature increased at the bearing-pad rings ahead of the temperature change between rings at the start of heat-up. This caused large axial temperature gradients on the pressure tube. The influence of adjacent bearing pads tended to limit the hot spot under the bottom bearing pads in weighted contact with the pressure tube. The local bearing-pad induced temperature of the pressure tube was only 10 to 35°C hotter than the bulk pressure-tube temperature at the bearing-pad ring, for the range of conditions studied in this program.

The bearing-pad heat-up rate increased and the pressure-tube heat-up rate decreased during the ballooning phase of most experiments. These changes indicated that the contact conductance between the bearing pad and the pressure tube decreased during the ballooning phase. Also, the change in contact conductance during ballooning was more pronounced when ballooning was accompanied by a significant change in pressure-tube wall thickness in the vicinity of the bottom bearing pads. The heat-up rate of the pressure tube between bearing-pad rings remained fairly constant during ballooning. This constant heat-up rate combined with the decreased heat-up rate at the bearing-pad ring resulted in a substantial reduction in the axial gradient on the pressure tube during the ballooning phase.

4.2 Post-test Observations

In eight of the nine experiments completed in this program, the pressure tube ballooned into contact with the calandria tube around the entire circumference and axially along the entire fuel element simulator heated length. The bundle sagged as a unit such that the bottom fuel element simulators remained in contact with the pressure tube during ballooning. The measured oxide thickness on the pressure tube was essentially unchanged from the autoclaved oxide thickness on the original pressure-tube section. The outside surface of the fuel element simulators and bearing pads, including the contacting surface of the bearing pad, had a black oxide coating after the experiments were completed. The post-test oxide thickness on the fuel element simulator cladding was less than 1 μm.

The pressure-tube segments used in these tests developed striations (circumferential waves aligned axially) on the outside and inside surfaces during ballooning contact with the calandria tube. These strain-induced striations were present even under the bottom bearing pads. The striations had the greatest amplitude in sections of the pressure tube that had the highest percentage of wall reduction during the ballooning phase. The stress magnitude also appears to affect the amplitude of the striations, since they were more pronounced in the 6 MPa tests than in the 3 MPa tests.

5. SUMMARY

The following observations were made from the experiments completed in this program:

1. The increase in local heat flux directly under the bottom bearing pads in weighted contact with the pressure tube was small. The resultant hot spots were not significant enough to cause local wall thinning under the bearing pads during ballooning.

2. The rate of heat transfer from the bearing pad to the pressure tube increased slightly before ballooning started, then decreased substantially during the ballooning phase.

3. Increased bundle power increased the differential temperature between the bearing pad and the pressure tube, but had minimal effect on the magnitude of the bearing-pad induced hot spot.

4. The resulting pressure-tube temperatures in the vicinity of the bottom bearing pads were similar for the "as-received" and the "T-pad" bearing pads. The hot spots under these pads were 10 to 15°C higher than the bulk pressure-tube temperatures. The "worn" bearing pad produced a hot spot approximately 35°C higher than the bulk pressure-tube temperature. This larger hot spot did not result in significant local pressure-tube wall thinning under this pad during the ballooning phase of the experiment.

The results from this experimental program will be used in computer codes (CATHENA, ABAQUS, ANSYS) to calculate values of contact conductance between the bearing pad and the pressure tube. These contact conductance values will be used to assess the influence of bearing-pad contact with the pressure tube in reactor safety analysis.

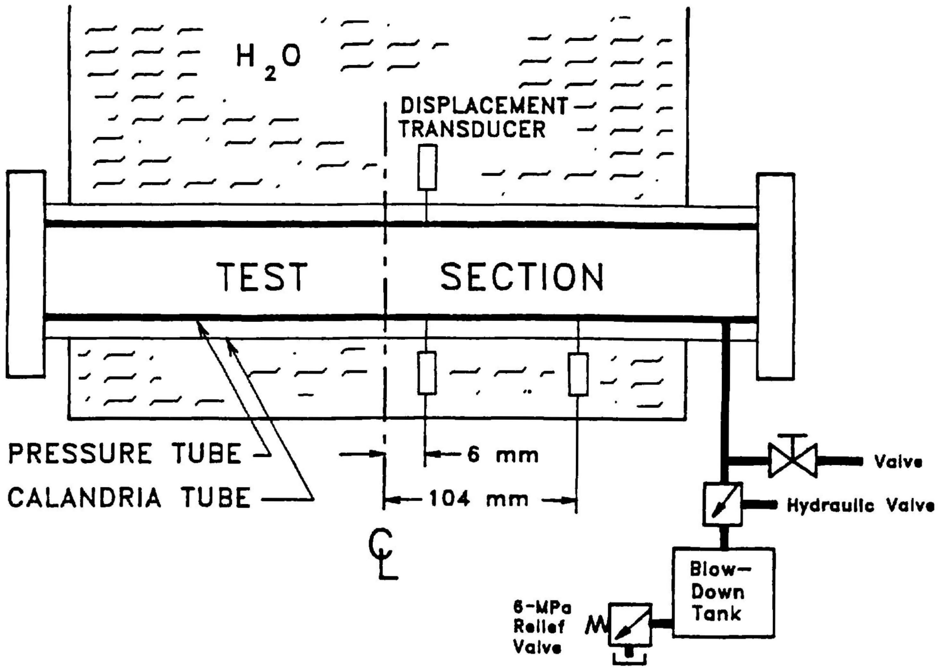

FIGURE 1. Schematic of Experimental Apparatus

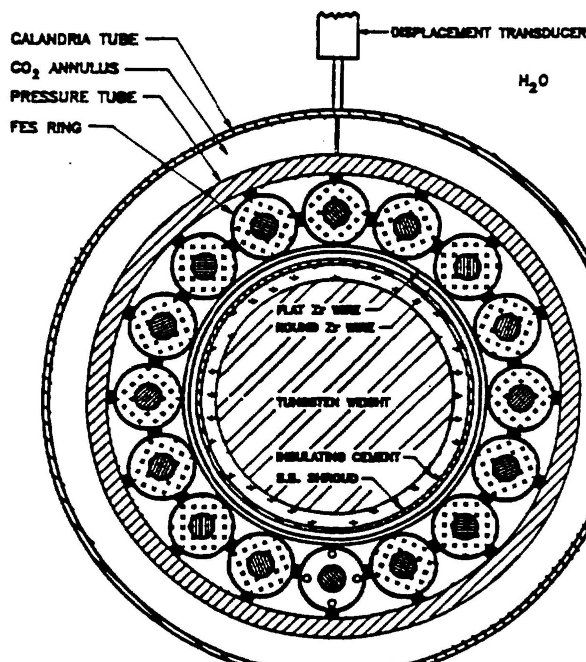

FIGURE 2. Cross-Section at the Centreline of the Test Section Showing Fuel Element Simulator (FES) Bundle Configuration

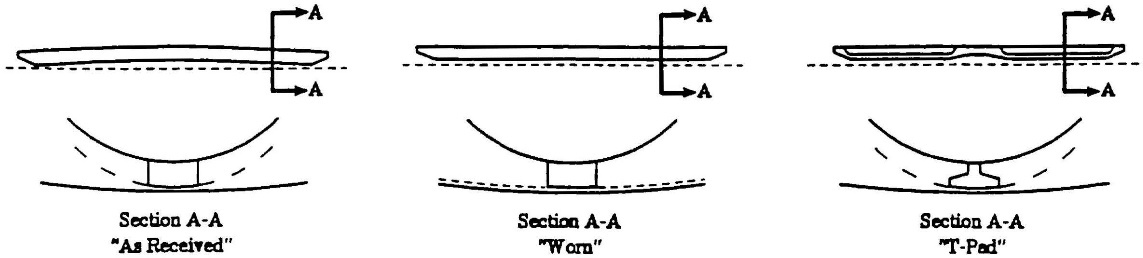

FIGURE 3. Bearing Pads at the Central Bearing-Pad Ring a) As-Received, b) Worn, and c) Modified T-Pad

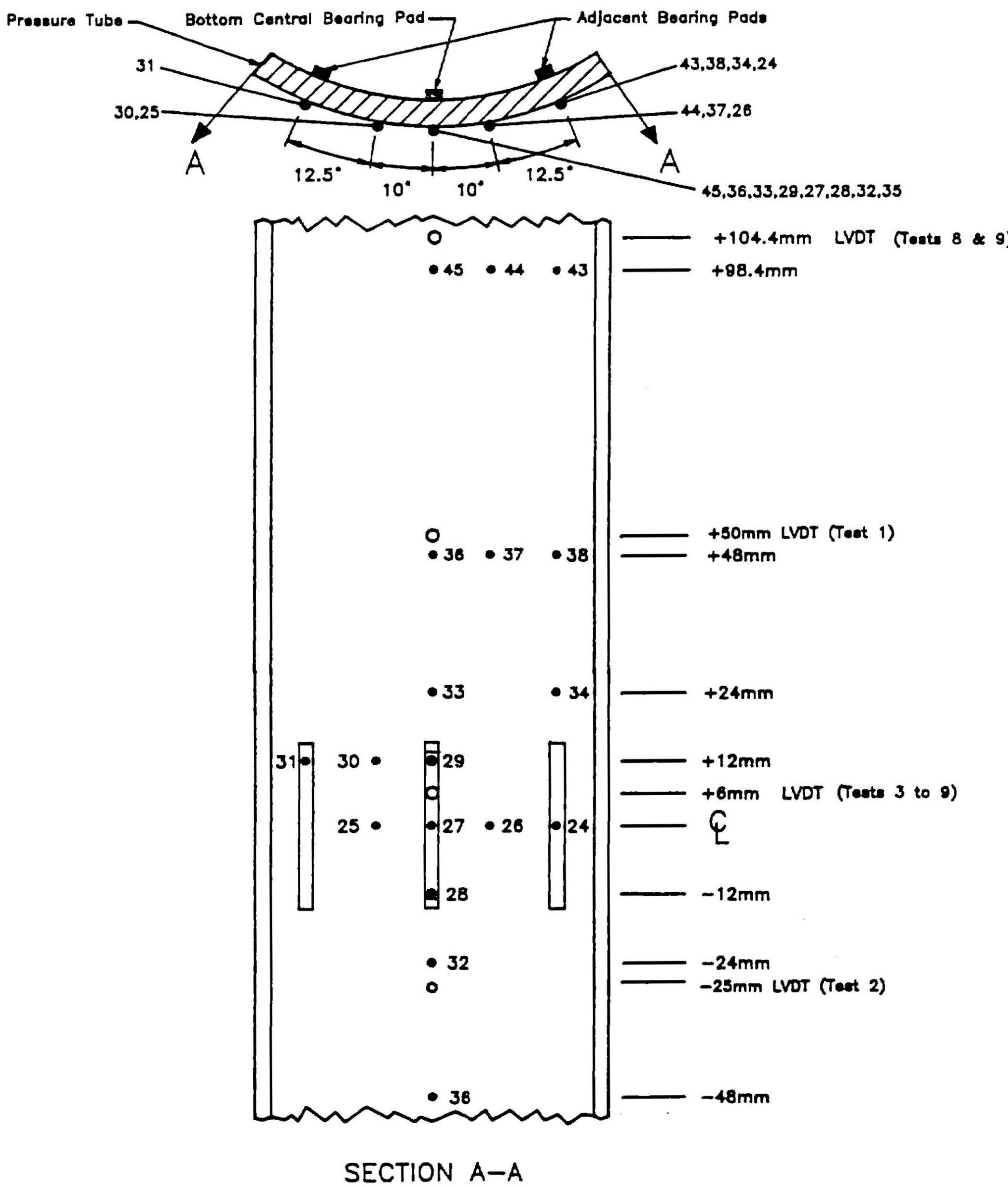

FIGURE 4. Typical Thermocouple Grid and Displacement Transducer (LVDT) Location on the Bottom of the Pressure Tube

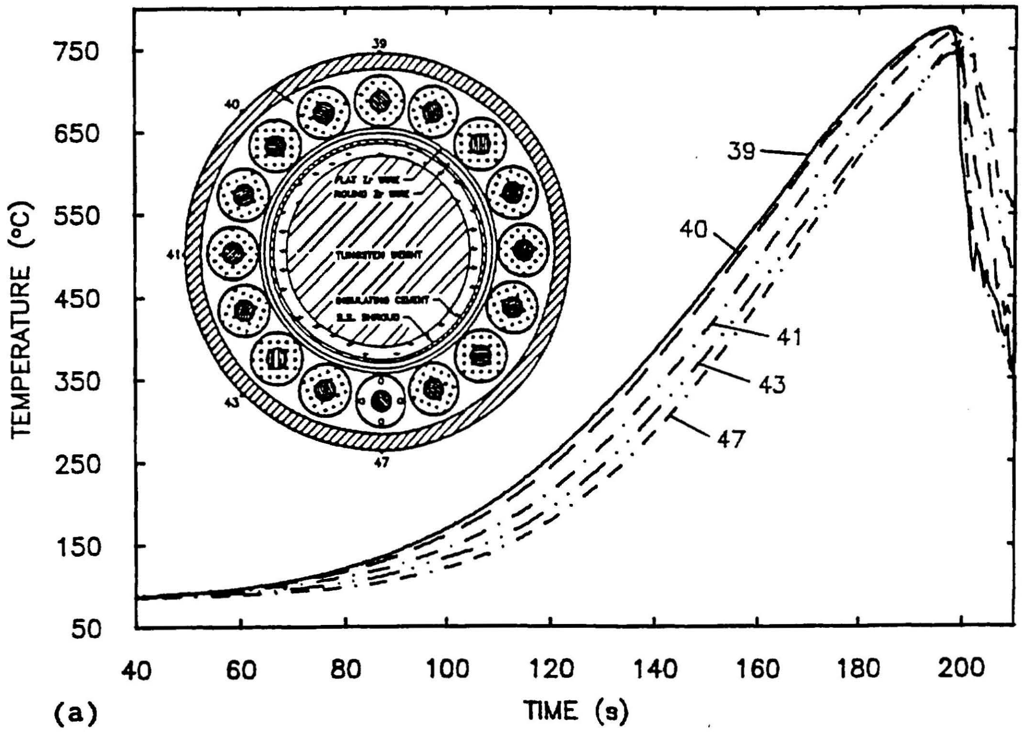

(a)

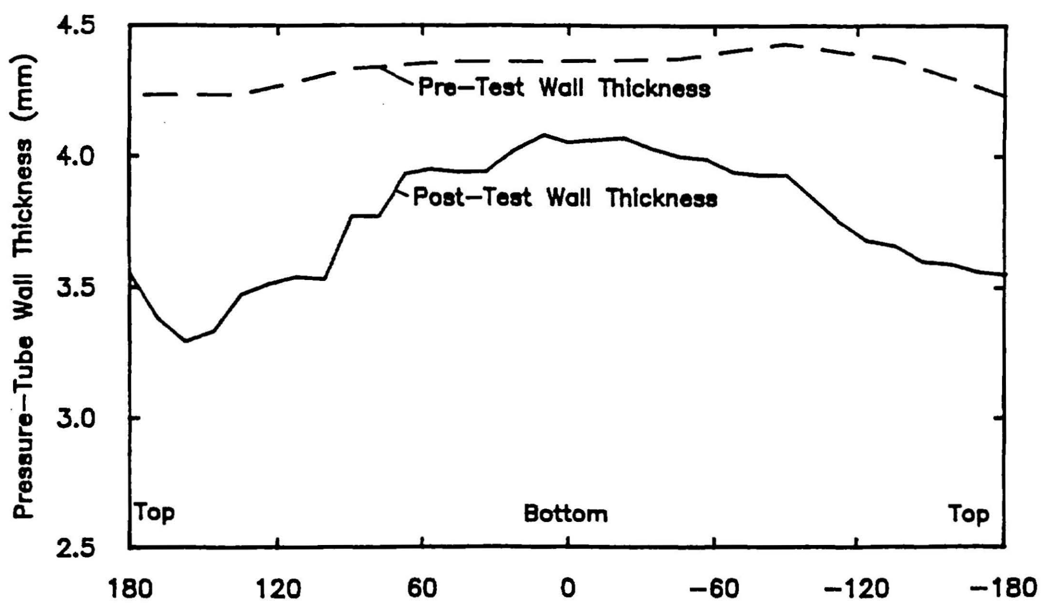

(b)

FIGURE 5. Circumferential Temperature Gradient on the Pressure Tube (a), and Wall Thickness of the Pressure Tube (b), in Test 7

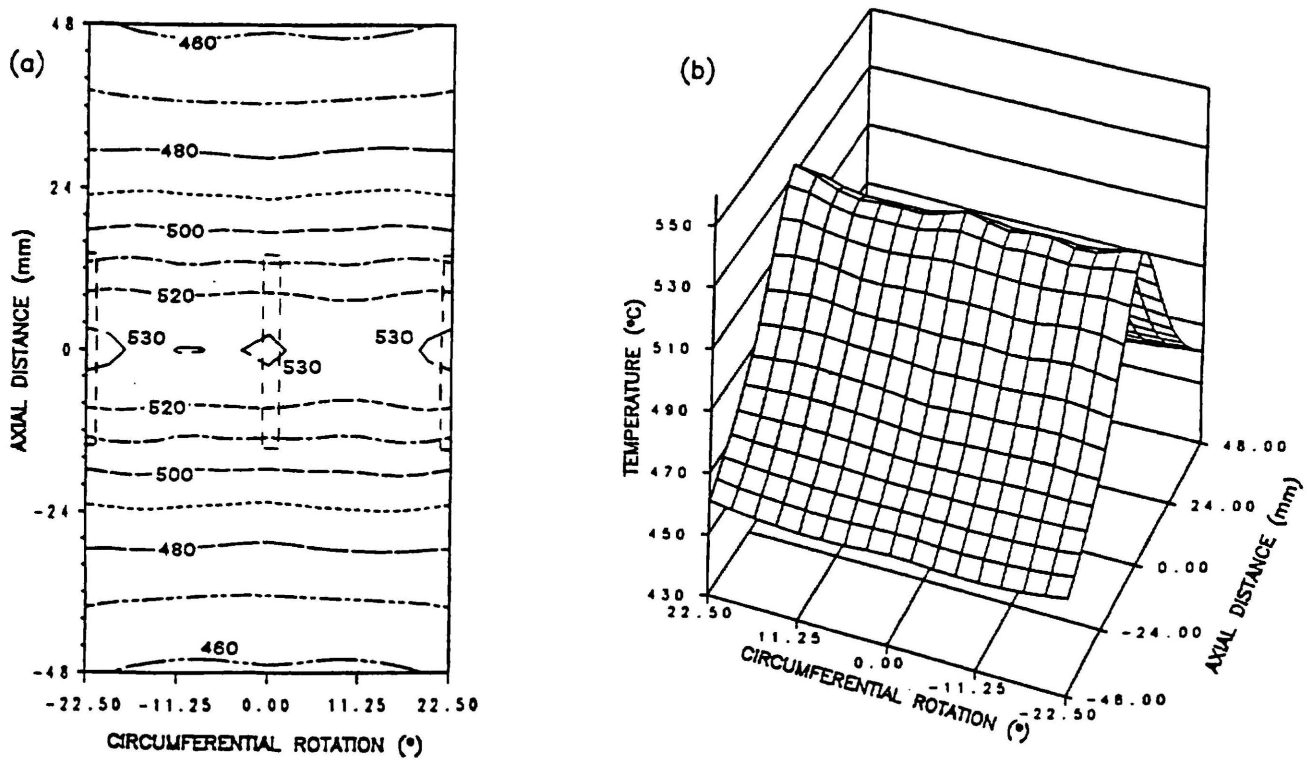

FIGURE 6: Two-Dimensional (a) and Three-Dimensional (b) Contour Plots From the Underside of the Pressure Tube During Mid-Heatup in Test 7 ("as-received" bearing pads), (temperatures in °C). The bottom three bearing pads are located at -22.5°, 0.0° and 22.5°.

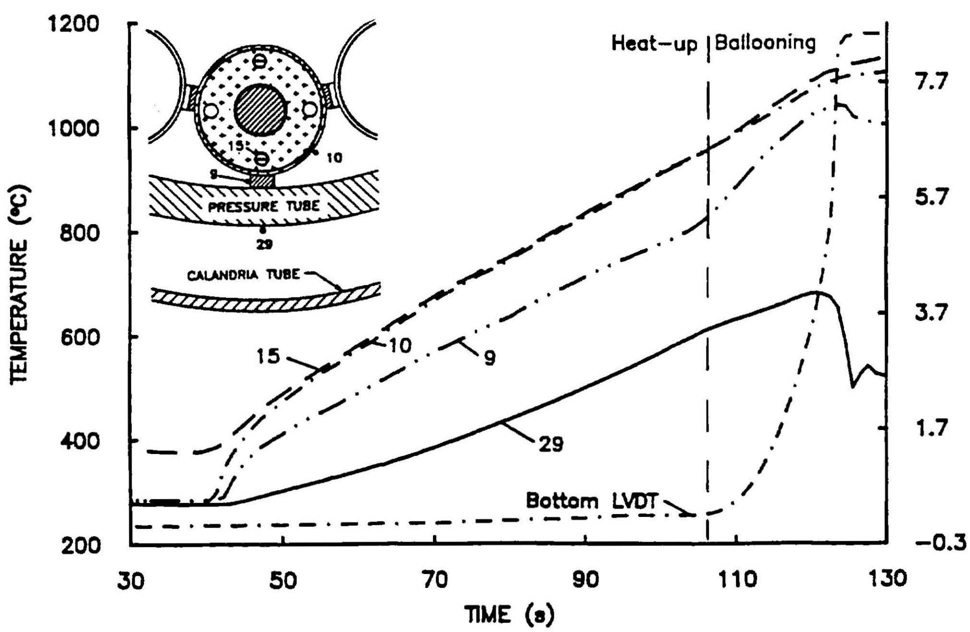

FIGURE 7. Thermal Gradient From Inside the Bottom Fuel Element Simulator to the Outside Surface of the Pressure Tube During Test 4. The displacement (bottom LVDT) of the pressure tube as it moved into contact with the calandria tube is also shown.

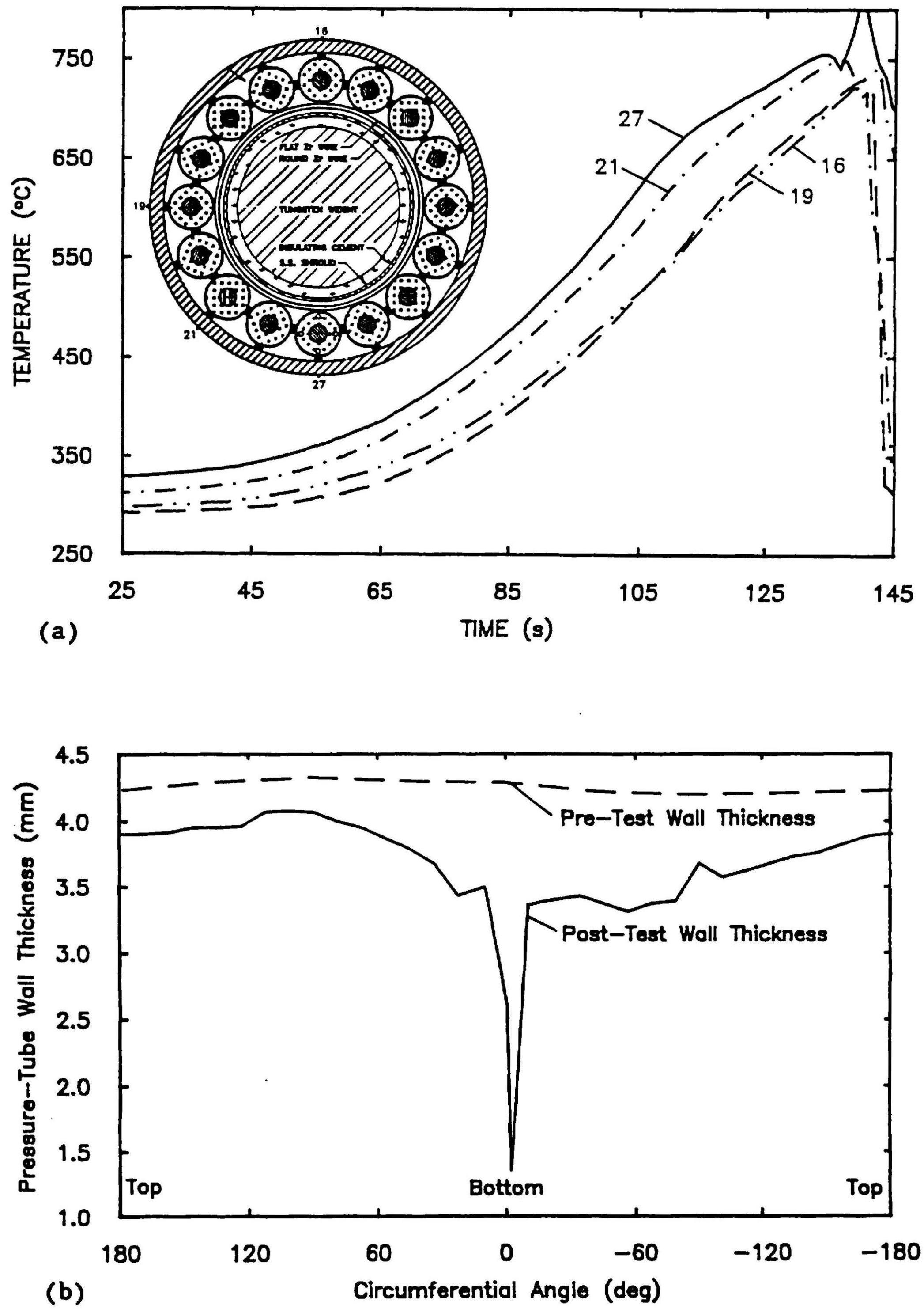

FIGURE 8. Circumferential Temperature Gradient on the Pressure Tube (a), and Wall Thickness of the Pressure Tube (b), in Test 5

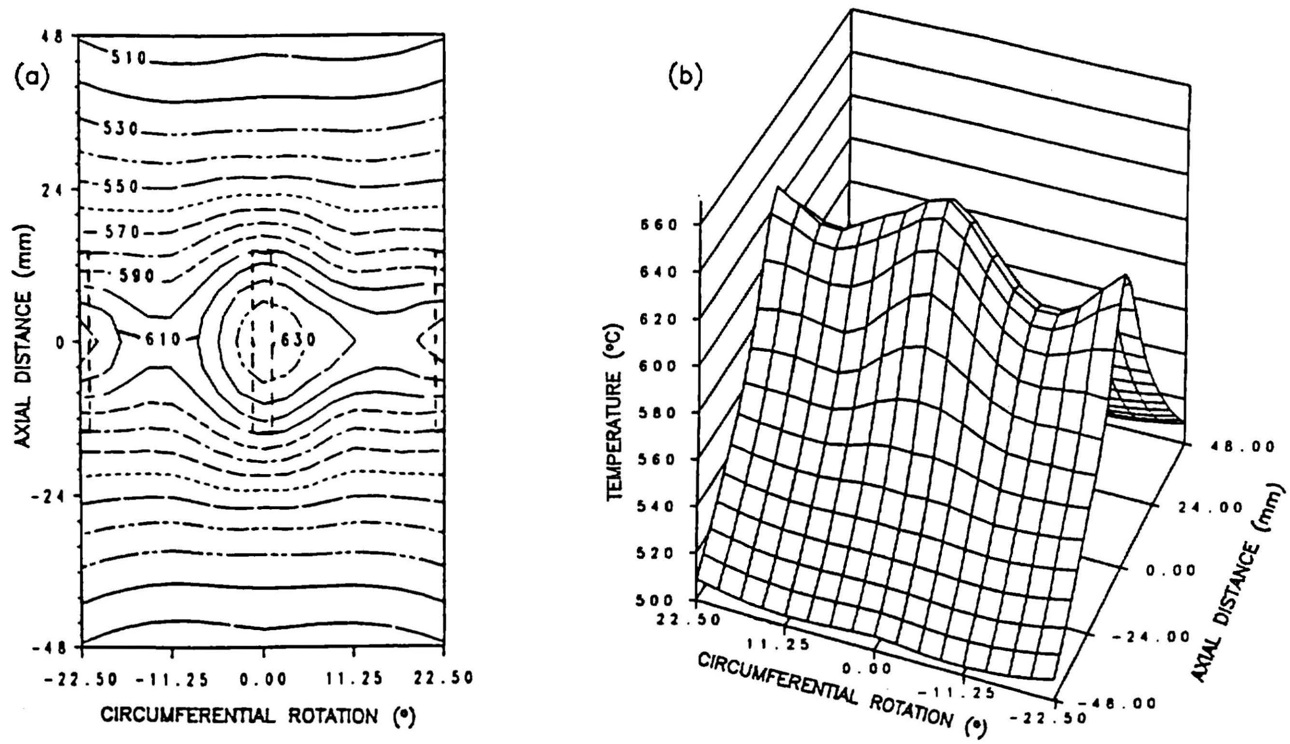

FIGURE 9: Two-Dimensional (a) and Three-Dimensional (b) Contour Plots From the Underside of the Pressure Tube During Mid-Heatup in Test 8 ("worn" bearing pads), (temperatures in ^{0}C). The bottom three bearing pads are located at -22.5^{0}, 0.0^{0} and 22.5^{0}.